Model analysis of thermal UV-cutoff effects on the chiral critical surface at finite temperature and chemical potential

Jiunn-Wei Chen, Hiroaki Kohyama, and Udit Raha

Phys. Rev. D **83**, 094014 — Published 13 May 2011

DOI: 10.1103/PhysRevD.83.094014

Model analysis of thermal UV-cutoff effects on the chiral critical surface at finite temperature and chemical potential

Jiunn-Wei Chen*
Department of Physics and Center for Theoretical Sciences, National Taiwan University, Taipei 10617, Taiwan

Hiroaki Kohyama†
Department of Physics, Chung-Yuan Christian University, Chung-Li 32023, Taiwan and Institute of Physics, Academia Sinica, Taipei 115, Taiwan and Physics Division, National Center for Theoretical Sciences, Hsinchu 300, Taiwan

Udit Raha‡
Department of Physics and Center for Theoretical Sciences, National Taiwan University, Taipei 10617, Taiwan

We study the effects of temporal UV-cutoff on the chiral critical surface in hot and dense QCD using a chiral effective model. Recent lattice QCD simulations indicate that the curvature of the critical surface might change toward the direction in which the first order phase transition becomes stronger on increasing the number of lattice sites. To investigate this effect on the critical surface in an effective model approach, we use the Nambu-Jona-Lasinio model with finite Matsubara frequency summation. We find that the nature of the curvature of the critical surface does not alter appreciably as we decrease the summation number, which is unlike the case what is observed in the recent lattice QCD studies. This may either suggest the dependence of chemical potential on the coupling strength or due to some additional interacting terms such as vector interactions which could play an important role at finite density.

PACS numbers: 12.38.Aw,11.10.Wx,11.30.Rd,12.38.Gc

I. INTRODUCTION

The study of the chiral critical point (CP) in the phase diagram of hot and dense quark matter is one of the central issues in Quantum Chromodynamics (QCD) [1]. While, it is widely accepted that the QCD phase transitions concerning chiral symmetry restoration and color deconfinement are crossovers with increasing temperature T for small chemical potential $\mu \simeq 0$, the order of the phase transitions along the μ direction for small T is still under considerable speculation. Model analysis indicate that a first-order phase transition occurs with increasing μ and for small T [2]. The above observations lead us to expect the existence of a critical point located at the end of the first order line in the phase diagram for some intermediate values, T_E and μ_E.

A first principle determination of the phase diagram by solving QCD itself is difficult due to the strongly interacting nature of matter at low-energies/temperatures which significantly restricts the range of applicability of perturbative calculations. We must then rely on non-perturbative techniques such as lattice QCD (LQCD) or some low-energy effective theories of QCD. The LQCD simulations are known to be a viable approach for microscopic calculations in QCD, and have recently reached a reliable level at finite T and $\mu = 0$ [3]. However, these simulations are not yet able to provide a conclusive understanding of the QCD phase diagram due to severe limitations posed by the well-known "sign-problem" at finite μ, and difficulties dealing with small quark masses, though only very approximate methods are available for simulations at small μ values [4]. Thus, it is important to develop low-energy effective models that may show consistency with lattice results and can be extrapolated into regions not accessible through simulations. Among them, the local Nambu-Jona-Lasinio (NJL) model [5] and its proposed extended version to include coupling of quarks to Polyakov-loops, the so-called Polyakov-loop NJL (PNJL) model [6], are useful to study the quark system at finite T and/or μ. Such effective models share the same symmetry properties of QCD and successfully describe the observed meson properties and chiral dynamics at low-energies (see, e.g., [7–10]).

Using the framework of (P)NJL model we search the CP and analyze the order of the chiral phase transition by varying the current quark masses (m_u, m_d, m_s). We usually set, for simplicity, $m_d = m_u$ and investigate the phase transitions in the m_u-m_s-μ space. Renormalization Group (RG) analysis of chiral models at $\mu \simeq 0$ conclude that there is no stable infra-red (IR) fixed-point for quark flavors $N_F > \sqrt{3}$ [11], indicating that the thermal phase transition is of fluctuation induced first or-

*Electronic address: jwc@phys.ntu.edu.tw
†Electronic address: kohyama@phys.sinica.edu.tw
‡Electronic address: udit.raha@unibas.ch; Present affiliation: Department of Physics and Astronomy, University of South Carolina, Columbia, SC 29208, USA

der for two or more flavors realized in the chiral limit $m_{u,d,s} = 0$. However, the transition becomes a crossover for intermediate quark masses because of explicitly broken chiral and center symmetries. Hence, it is naturally expected that there should be a "critical boundary" separating the regions of the first order phase transition and crossover between small and intermediate quark masses. Although LQCD results support the above model picture qualitatively, there had been a huge quantitative difference between the two kinds of analyses, even at zero chemical potential where the LQCD does not suffer from the sign-problem; the value of the critical mass obtained in the (P)NJL model is about one order of magnitude smaller than the value in the LQCD analyses. Inspired by recent works reporting that the critical mass may become smaller when the number of lattice sites is increased [12, 13], the present authors studied the critical boundary in the (P)NJL model with finite Matsubara frequency summation N at zero chemical potential [14]. There it was found that the critical mass actually becomes larger if one decreases the Matsubara summation number N (see, Eq.(7)), thereby showing the correct tendency to explain the quantitative difference between the LQCD and (P)NJL model results.

In this Letter, our goal is to study the critical boundary for all values of the chemical potential, which may eventually tell us the location of the CP in the QCD phase diagram. As already mentioned that since an *ab initio* determination of the critical point in QCD is a distant hope, nevertheless, it is worth studying the (P)NJL model with finite frequency summation at finite chemical potential that should capture the essential qualitative features of the results expected in lattice studies. Note that in the m_u-m_s-μ space, the critical boundary becomes a surface called the "critical surface". More precisely, through this study we would like to investigate the qualitative behavior of this critical surface whose shape can critically determine whether the CP exists. We can then compare our results with the recent lattice predictions.

II. MODEL SET UP

The NJL model Lagrangian in the 3 flavor system is written by

$$\mathcal{L}_{\rm NJL} = \bar{q}\,(\mathrm{i}\partial\!\!\!/ - \hat{m})\,q + \mathcal{L}_4 + \mathcal{L}_6, \tag{1}$$

$$\mathcal{L}_4 = \frac{g_{\rm S}}{2}\sum_{a=0}^{8}\left[(\bar{q}\lambda_a q)^2 + (\bar{q}\,\mathrm{i}\gamma_5\lambda_a q)^2\right], \tag{2}$$

$$\mathcal{L}_6 = -g_{\rm D}\left[\det \bar{q}_i(1-\gamma_5)q_j + \text{h.c. }\right]. \tag{3}$$

Here $\hat{m}$ is the diagonal mass matrix (m_u, m_d, m_s) in the flavor space which explicitly breaks the chiral symmetry. $\mathcal{L}_4$ is the 4-fermion contact interacting term with coupling constant $g_{\rm S}$, and λ_a is the Gell-Mann matrix in the flavor space with $\lambda_0 = \sqrt{2/3}\,\mathrm{diag}(1,\,1,\,1)$. $\mathcal{L}_6$ is a 6-fermion interaction term called the Kobayashi-Maskawa-t'Hooft interaction whose coupling strength is $g_{\rm D}$ [15]. The subscripts $(i,\,j)$ indicate the flavor indices and the determinant runs over the flavor space. This term is introduced to explicitly break the $\mathrm{U_A}(1)$ symmetry.

To study the chiral dynamics, we solve the gap equations which are derived through differentiating the thermodynamic potential Ω by the order parameters of the model:

$$\frac{\partial\,\Omega}{\partial\,m_i^*} = 0 \quad ; \quad i = u, d, s \tag{4}$$

The order parameters m_i^* are the constituent quark masses. Since, we set $m_d = m_u$ in our analysis, this should lead to the isospin symmetric result $m_d^* = m_u^*$, reducing the number of gap equations from three to two. The thermodynamic potential Ω is defined by $\Omega \equiv -\ln Z/(\beta V)$, where Z is the partition function, $\beta(\equiv 1/T)$ is the inverse temperature and V is the volume of the thermal system.

In the mean-field approximation, after some algebra, we arrive at the following expressions for the gap equation:

$$\begin{aligned} m_u^* &= m_u + 2\mathrm{i}\,g_{\rm S}\,N_c\mathrm{tr}S^u - 2g_{\rm D}N_c^2(\mathrm{tr}S^u)(\mathrm{tr}S^s), \\ m_s^* &= m_s + 2\mathrm{i}\,g_{\rm S}\,N_c\mathrm{tr}S^s - 2g_{\rm D}N_c^2(\mathrm{tr}S^u)^2, \end{aligned} \tag{5}$$

where $N_c(=3)$ is the number of colors and $\mathrm{tr}S^i$ is the chiral condensate written explicitly as

$$\mathrm{i}\,\mathrm{tr}S^i = 4m_i^*\int\frac{d^3p}{(2\pi)^3}\,(\mathrm{i}\,T)\sum_{n=-\infty}^{\infty}\frac{\mathrm{i}}{(\mathrm{i}\,\omega_n)^2 - E_i^2}\,. \tag{6}$$

Here $w_n = \pi T(2n+1)$ is the Matsubara frequency and $E_i = \sqrt{\mathbf{p}^2 + m_i^{*\,2}}$ is the energy of the quasi-particle. A detailed calculation for deriving the gap equations Eq.(5) is clearly presented in the review paper [8].

To study the UV-cutoff effects in the model, we cut the higher frequency modes in the Matsubara sum as employed in [14],

$$\sum_{n=-\infty}^{\infty} \longrightarrow \sum_{n=-N}^{N-1}. \tag{7}$$

This model has five free parameters $\{m_u,\,m_s,\,\Lambda,\,g_{\rm S},\,g_{\rm D}\}$: two current quark masses, a 3-dimensional momentum cutoff, a four-fermion and a six-fermion coupling constants. Following [7], we set $m_u = m_u^{\rm phys} = 5.5$MeV fixed for all values of N, while the remaining four parameters are fitted each time by using the following physical observables

$$\begin{aligned} m_\pi &= 138\text{ MeV}, & f_\pi &= 93\text{ MeV}, \\ m_K &= 495.7\text{ MeV}, & m_{\eta'} &= 958\text{ MeV}. \end{aligned}$$

The parameter fitting for various N has been done in [14], and we employ the same values in this analysis which are again displayed in Tab. I for the convenience of the reader.

N	m_s (MeV)	Λ (MeV)	$g_{\rm S}\Lambda^2$	$g_{\rm D}\Lambda^5$
15	134.7	631.4	4.16	12.51
20	135.0	631.4	4.02	11.56
50	135.3	631.4	3.82	10.14
100	135.4	631.4	3.75	9.69
∞	135.7	631.4	3.67	9.29

TABLE I: The various fitted parameters for different N [14].

III. CHIRAL CRITICAL SURFACE

The main purpose of this Letter is to determine the chiral critical surface in the (P)NJL model with finite Matsubara summation. The critical surface is the set of all critical points in the m_u-m_s-μ space which are analyzed by scanning the space for discontinuities of the chiral condensate. It should be noted that for each value of N, we treat both the current quark masses m_u and m_s as free parameters in obtaining the critical surface once the other parameters, namely, Λ, $g_{\rm S}$ and $g_{\rm D}$ are determined by fitting to the physical parameters, as shown in Tab. I. Of course, we will eventually be interested in the case of the real (physical) current quark masses $m_u^{\rm phys} \simeq 5.5$MeV and $m_s^{\rm phys} \simeq 135$MeV, in order to determine the possible existence/non-existence of the CP through our model analysis. Because our motivation is to make a direct comparison of our results with that of LQCD where the simulations are mainly performed in the $m_u = m_s$ symmetric case at finite μ, we shall also consider this case. In the actual numerical calculations, we scouted out the critical masses (m_{uc},m_{sc}) for each μ by searching for discontinuities in the solutions of the gap equations Eq.(5) in the entire m_u-m_s-μ space, in general.

The LQCD and model studies indicate a crossover realized at $\mu = 0$ for physical current quark masses. This means that the curvature of the critical surface will tell us whether the CP is favored in the phase diagram. To be more concrete, if the region of the first order phase transition expands with increasing μ, the physical quark mass line will intersect with the critical surface and this will end up as a CP. If on the other hand, the first order phase transition region shrinks with μ, there is less chance of an appearance of a the CP and a crossover transition will be favoured for the whole range of T and μ. Thus the sign of the curvature is indeed important, and the main purpose of this Letter is to study whether the sign can change by decreasing N from the usual case of $N = \infty$.

In the LQCD calculations, the curvature of the critical surface along the $m_u = m_s$ symmetric line is analyzed by obtaining the critical mass m_c as a function of the ratio of the critical chemical potential μ_c and the critical temperature T_c, through the following Taylor expansion formula

$$\frac{m_c^N(\mu_c)}{m_c^N(\mu_c=0)} = 1 + \sum_{k=1} c_k^N \left(\frac{\mu_c}{\pi T_c}\right)^{2k}, \qquad (8)$$

which so far yielded the following results: $c_1^4 = -3.3(3)$, $c_2^4 = -47(20)$ for $N_t = 4$, and $c_1^6 = 7(14)$, $-17(18)$ (preliminary) for a leading order (LO) and next-to-leading order (NLO) extrapolation in μ^2, respectively, for $N_t = 6$ where N_t represents the number of the lattice sites in the temporal direction [13]. These results are graphically represented in Fig. 3 and 6 in the following sections which indicate that the sign of the curvature has not yet been determined from lattice simulations.

IV. NJL MODEL RESULTS

In this section, we demonstrate the numerical methodology in obtaining the phase diagram and chiral critical surface for the NJL model.

A. Phase diagram

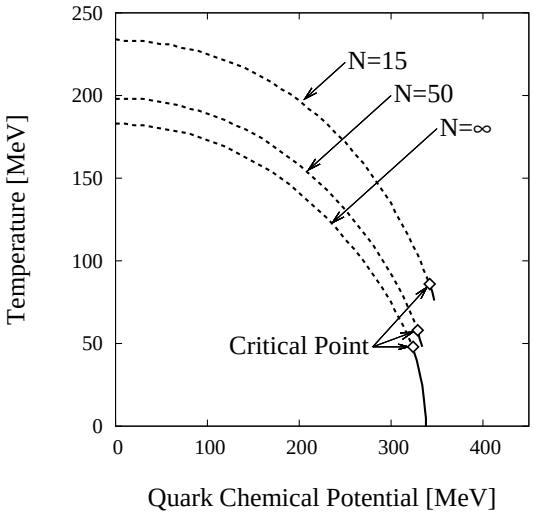

FIG. 1: Position of the CPs on the T-μ phase diagrams from the NJL model with finite Matsubara summation and the current quark masses being equal to the respective physical quark masses obtained by fitting for $N = 15, 50, \infty$. The dotted and the solid lines represent crossovers and first order phase transitions, respectively. The $N = \infty$ case corresponds to the traditional NJL model.

In in Fig. 1, we display the phase diagrams for simulations at the physical quark mass values of the current current quarks obtained from fitting for $N = 15$, 50 and ∞, respectively. Here we use the parameters shown in Tab. I where m_u is kept fixed at 5.5MeV and m_s is around 135MeV. We have also studied the model for other values of N, however, there were no significant qualitative differences and we prefer to select just the above three representative cases for graphical clarity. Here, it may be noteworthy mentioning that for values of $N < 15$, it becomes a matter of numerical challenge to perform simulations to determine the phase boundaries. So, henceforth,

we shall be displaying our results only for the above three cases. Note that the case $N = \infty$ corresponds to the traditional NJL model. In drawing the phase diagrams, we apply the same criterion employed in [10] where the phase transition or crossover is defined by the condition,

$$\left.\frac{\langle\bar{u}u\rangle}{\langle\bar{u}u\rangle_{T_0}}\right|_{T=T(\mu)} = \frac{1}{2}, \tag{9}$$

$\langle\bar{u}u\rangle_{T_0}$ being the expectation value of the chiral condensate for the up quark at temperature T_0 and $\mu = 0$. We choose $T_0 = 0$ for the $N = \infty$ traditional model, while we set $T_0 = 50$MeV for the case with finite N since the model is ill-defined for small T, as discussed in [14]. This is why we choose not to display the results for the small T region where the curves are no longer physically reliable.

Here it is seen that the region below each of the curves that represents the chiral symmetry broken phase expands with decreasing N. This comes from the fact that the coupling constants become larger with decreasing N, being consistent with RG arguments that the coupling strength becomes smaller when one considers the physics at higher momenta, i.e., for larger N. When the coupling strength grows the chiral condensate tends to enlarge, which can be easily seen from Eq.(5). Thus, it is naturally understood why the transition temperature increase with a smaller choice of the summation number N.

Before proceeding to the critical surface, let us discuss how the phase diagram varies with changing current quark masses. Since we treat the current quark masses as free parameters in drawing the critical surface, it is worth displaying the phase diagrams for different current quark masses, as shown in Fig.2 for the case $N = \infty$. Here in particular, we have chosen the $m_u = m_s (\equiv m)$ symmetric direction to get a general idea of the nature of phase diagram.

We see that the CP moves towards lower μ and higher T with decreasing m, and it eventually hits $\mu = 0$ axis at $m = 1.1$MeV. For small current quark masses the order of the transition is of the first, which is consistent with the symmetry arguments presented in [11]. This suggests that the critical chemical potential μ_c and the critical temperature T_c could be thought of as functions of the current quark masses, or conversely, one can express the critical mass m_c as a function of μ_c and T_c, namely, $m_c(\mu_c, T_c)$, or equivalently, $m_c(\mu_c/\pi T_c)$. This leads to the very idea of the chiral critical surface or the Columbia plot which is our central issue. Note that for other values of N, although the region of the broken phase expands with decreasing N, the qualitative behavior seen above in Fig.2 is found to be more or less the same.

For the sake of comparison with the LQCD Taylor expansion formula Eq.(8), we define the following function $R(N, x)$

$$R(N,x) \equiv \frac{m_c^N(x)}{m_c^N(x=0)} = 1 + \sum_{k=1} c_k^N x^{2k}, \tag{10}$$

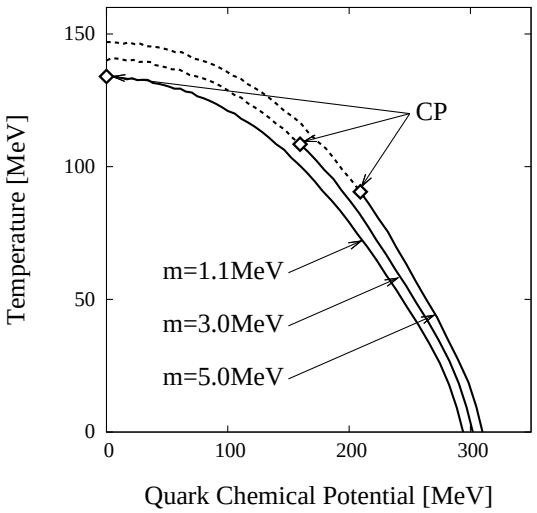

FIG. 2: Position of the CP in the phase diagrams from the traditional $N = \infty$ NJL model with $m(= m_u = m_s) = 1.1$, 3, 5MeV. The dotted and the solid lines represent crossovers and first order phase transitions, respectively.

with $x = \mu_c/\pi T_c$. Thus the ratio of the critical mass m_c can be written as the function of N and x. For example, $m_c^N(0)$ takes the values 1.1, 1.3 and 2.2MeV, respectively, for $N = \infty$, 50 and 15, and hence $m_c^N(0)$ is strongly N dependent. It may also be worth showing the corresponding values of T_c in above three cases: $T_c = 135$, 153 and 190MeV for $N = \infty$, 50 and 15.

B. Critical surface

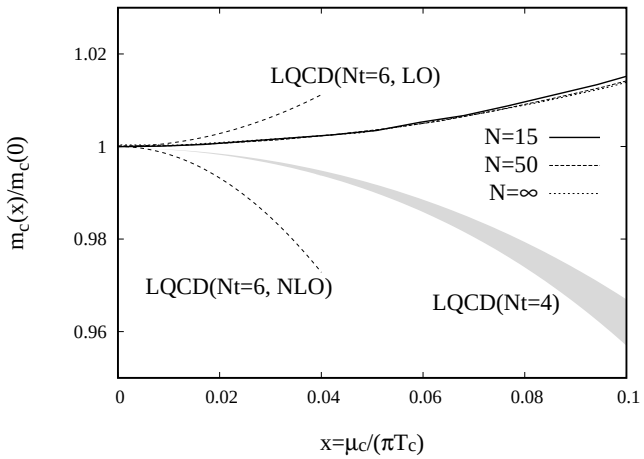

FIG. 3: $m_c^N(x)/m_c^N(0)$ vs $x(= \mu_c/\pi T_c)$ plot for different N values from the NJL model, along with the corresponding results obtained from lattice simulations for $N_t = 4$ and $N_t = 6$. The actual values of $m_c^N(0)$ are 1.1, 1.3 and 2.2MeV for $N = \infty$, 50 and 15, respectively.

In Fig. 3, we show the numerical results for $m_c^N(x)/m_c^N(0)$ as a function of $x(=\mu_c/\pi T_c)$, along with the corresponding results obtained in the recent LQCD simulations for $N_t = 4$ and 6 [13], respectively. We see that the slope of the curves tends to go up only very slightly on decreasing N from $N = \infty$ down to $N = 15$. On the other hand, the results from lattice simulations do not yield conclusive results so far, as clearly revealed from the above figure, where the sign of the curvature has not yet been constrained for the $N_t = 6$ case. Thus, in comparison with the lattice studies, we find that the qualitative behavior of our model results hardly changes by using different N values in our analysis. This means that there is indeed a stark quantitative contrast between the NJL model results and the lattice predictions.

One particular aspect of the above results deserve a closer inspection: here we draw Fig. 3 based on the idea of Eq.(10) in which the N dependence of the curvature comes from the coefficients c_k^N. The slope critical curves as seen in Fig. 3 has a negligible N dependence for small x, which mean that, if we were to assume a numerical expansion as Eq.(10) applicable to the critical curves, c_k^N for small k would be nearly independent of N as well. A splitting of the curves indeed takes place on increasing to large x when some N dependence may creep in for larger k values. However, although there appears some deviations for higher x (or μ), the qualitative behavior of the critical surface does not change appreciably with N at least for up to some $\mu(\sim 300\text{MeV})$ as we shall see below.

We are now in the position to actually display our results for the chiral critical surface on the Columbia plot for the general case of real current quark masses. In Fig. 4, we display our results obtained for the $N = \infty$ and 15 cases. It is clearly seen that, although the values of the critical mass changes about factor of two, the slope of the curvature does not differ as we change the value of N. Thus, the region of the first order phase transition expands with respect to μ for all N values, since the effect of variation of N is rather too nominal to change the sign of the curvature of the critical surface. This would then mean that the NJL model will always favour the CP with physical current quark masses at some finite value of μ, e.g., we obtain the CP when μ goes up around $\mu_c = 324\,(342)$ MeV for $N = \infty\,(15)$, as exhibited in the phase diagram Fig. 1.

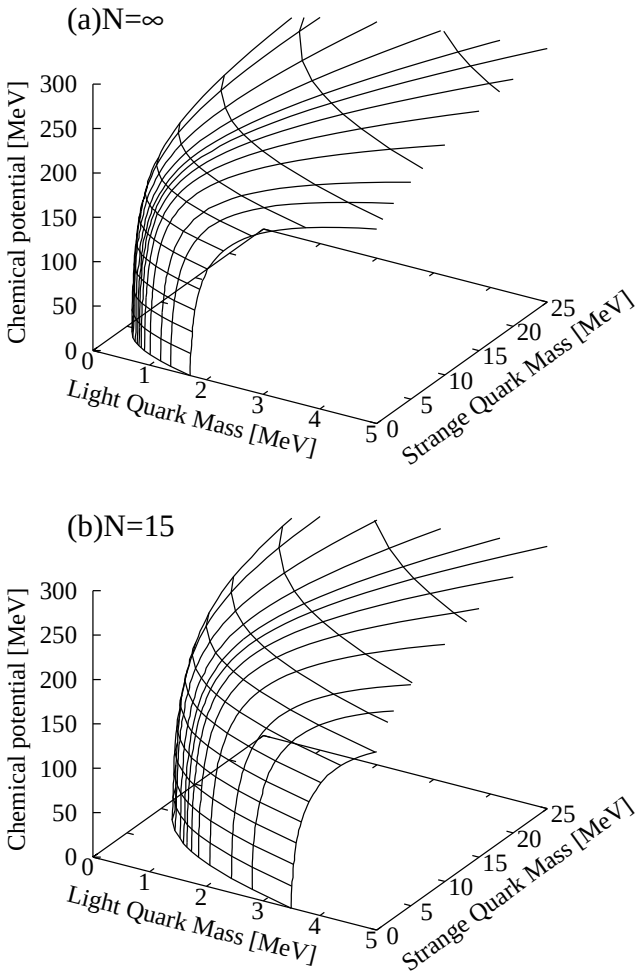

FIG. 4: The chiral critical phase surfaces for (a) $N = \infty$, and (b) $N = 15$ from the NJL model in the m_u-m_s-μ space.

V. THE PNJL MODEL EXTENSION

It is also intriguing to study the critical surface in the PNJL model, because of the closer resemblance to QCD which treats the chiral and deconfinement phase transitions simultaneously. In the PNJL model, the order parameter for the deconfinement phase transition is the Polyakov-loop and it is described by a global mean-field being similar to the chiral condensation in the traditional NJL model. The Lagrangian of the PNJL model is written as [10],

$$\mathcal{L}_{\rm PNJL} = \mathcal{L}_0 + \mathcal{L}_4 + \mathcal{L}_6 + \mathcal{U}(\Phi, \Phi^*, T)\,, \tag{11}$$

$$\mathcal{L}_0 = \bar{q}\,(\mathrm{i}\partial\!\!\!/ - \mathrm{i}\gamma_4 A_4 - \hat{m})\,q\,, \tag{12}$$

$$\mathcal{U}(\Phi, \Phi^*, T) = -bT\big\{54\,\mathrm{e}^{-a/T}\Phi\Phi^* + \ln\big[1 - 6\Phi\Phi^* + 4(\Phi^3 + \Phi^{*\,3}) - 3(\Phi\Phi^*)^2\big]\big\}\,, \tag{13}$$

where $\mathcal{U}$ is the Polyakov-loop effective potential and Φ and Φ^* are the traced Polyakov- and the anti-Polyakov-loop, respectively. They are defined by $\Phi = (1/N_c)\mathrm{tr}L$, $\Phi^* = (1/N_c)\mathrm{tr}L^\dagger$ with $L = \mathcal{P}\exp[\mathrm{i}\int_0^\beta \mathrm{d}\tau A_4]$ and $A_4 = \mathrm{i}A^0$. There are several candidates for the Polyakov-loop potential in defining the PNJL model [6, 10, 17], and we adopt the strong-coupling inspired form of Eq.(13) following [10]. In the above expressions, the parameter a solely parametrizes the strength of the Polyakov-loop condensate for the deconfinement phase transition, while the parameter b controls the relative strength of the mixing between the Polyakov-loop and chiral condensates,

with a smaller value of b signifying chiral phase transition dominating over deconfinement. Here, the parameters a and b are set as $a = 664$ MeV, and $b \cdot \Lambda^{-3} = 0.03$. Regarding the rest of the model parameters, it is legitimate to use the same ones fixed in the NJL model because the Polyakov-loop extension is likely to affect the system only at finite temperatures comparable to the critical temperature T_c. At much lower temperatures the chiral condensate is only very marginally modified by the Polyakov loops.

VI. PNJL MODEL RESULTS

Let us now discuss the results in the PNJL model with finite frequency summation.

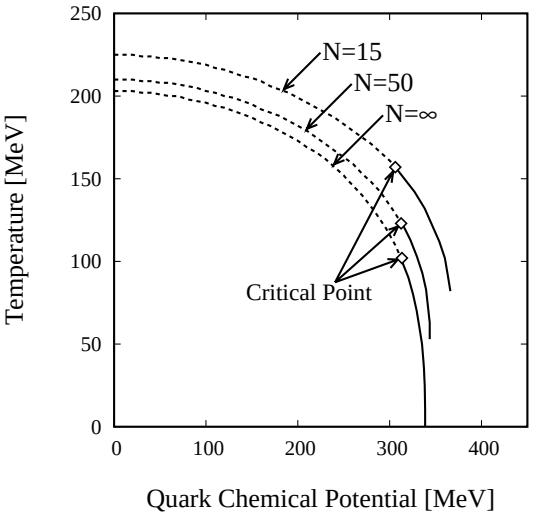

FIG. 5: Position of the CP on the T-μ phase diagrams from the PNJL model with finite Matsubara summation and the current quark masses being equal to the respective physical quark masses obtained by fitting for $N = 15$, 50, ∞. The dotted and the solid lines represent crossovers and first order phase transitions, respectively. The $N = \infty$ case corresponds to the traditional PNJL model.

In Fig. 5, we present the phase diagrams resulting from the PNJL model at physical quark masses with $N = 15$, 50 and ∞. Here we see that the curves are very similar to the ones in Fig. 1, however, the critical temperatures are about a factor of two or more larger than those obtained via the NJL model. This is almost the same quantitative difference as is observed between the traditional ($N = \infty$) NJL and PNJL models [18].

We again display the corresponding curves for the ratio $m_c^N(x)/m_c^N(0)$ and compare the results with the LQCD simulations in the small ($x < 0.1$) region. We see that the nature of the results exhibit similar qualitative characteristics with the ones obtained in the NJL model; the ratio does not change appreciably, although $m_c^N(0)$ is strongly dependent on N. However, the ratios are numerically

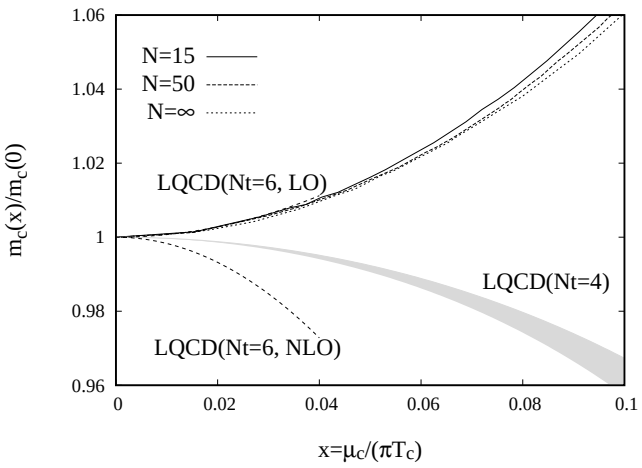

FIG. 6: $m_c^N(x)/m_c^N(0)$ vs $x(= \mu_c/\pi T_c)$ plot for different N values from the PNJL model, along with the corresponding results obtained from lattice simulations for $N_t = 4$ and $N_t = 6$. The actual values of $m_c^N(0)$ are 1.3, 1.6 and 2.6MeV for $N = \infty$, 50 and 15, respectively.

larger than that obtained with the NJL case. This result can be interpreted as an effect of the Polyakov-loops tending to suppress unphysical quark excitations below T_c [10].

Finally, in Fig. 7, the critical surfaces in the PNJL model with $N = \infty$ and 15 are displayed. We confirm that the region of the first order transition expands with respect to μ in these two figures, quite similar to that found previously in the NJL case. It is interesting to note that such qualitative similarity between the NJL and PNJL model results is *a priori* non-trivial, since the deconfinment phase transition order parameters, namely the Polyakov-loops Φ and Φ^*, respectively, may cause the system with chiral and deconfinment phase transitions to deviate significantly (both qualitatively and quantitatively) from a system with only chiral phase transition, especially in the vicinity of the CP.

VII. SUMMARY AND DISCUSSION

In this Letter, we studied the UV-cutoff effects on the chiral critical surface with two light and one heavy flavors using the (P)NJL model. We found that although the critical masses may strongly depend on the choice of N, the "normalized" critical surface, denoted by the function $R(N, x)$, is not appreciably affected on changing N while restricting to the small x region where lattice simulation data is currently available. Note, however, that there appears a nominal deviation for larger x. Our general conclusion is that the critical surfaces show rapidly expanding behavior for high μ, namely at high x, as clearly evident from Figs. 4 and 7, in which case the "physical" line corresponding to the physical current quark

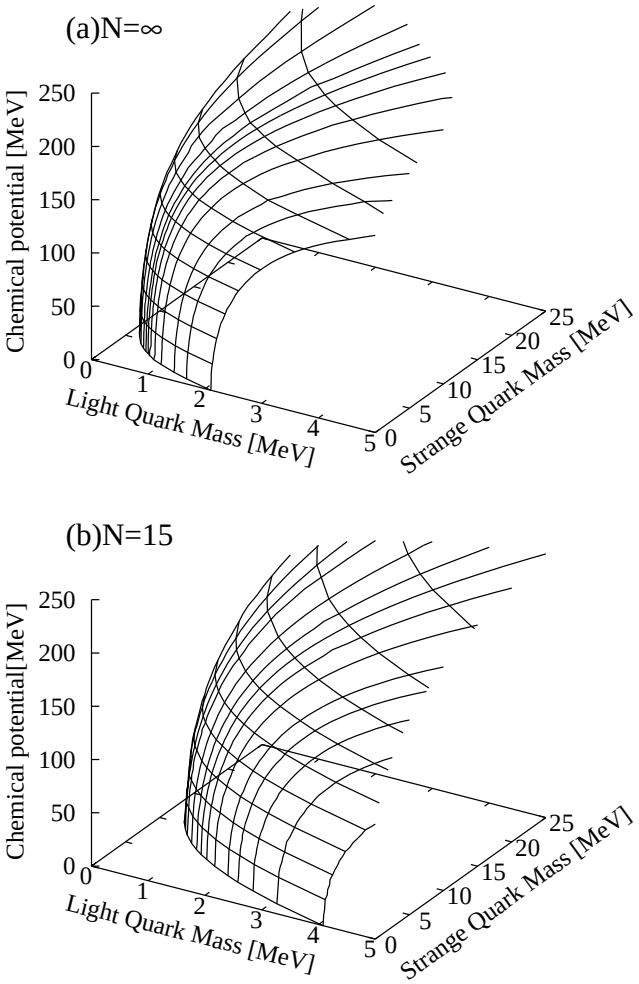

FIG. 7: The chiral critical phase surfaces for (a) $N = \infty$, and (b) $N = 15$ from the PNJL model in the m_u-m_s-μ space.

mass lines always intersects the critical surface due to its monotonically expanding nature. In other words, the NJL model always seems to favor the existence of the CP scenario, irrespective to choice of N. While, on the other hand, the current lattice simulations are not decisive at the moment being beset with larger lattice cut-off effects than finite density effects, making continuum extrapolations doubtful. However, there is still room for further precise lattice calculations in future with greater number of lattice sites and development of new techniques for finite-density simulations that may be necessary to make definite conclusions.

As a final note, we point out the possibility of the temperature and density dependence of the coupling constants that may become important at high-energies, as we expect the couplings to run with respect to the energy scale. However, to test the effects of the temporal UV-cutoff, we have used constant values of the couplings $g_{\rm S}$ and $g_{\rm D}$ which were fixed from the very outset by fitting to physical quantities at small temperature and chemical potential. These dependencies so arising may turn out to have crucial effects on the critical surface especially when considering the system at high densities, where it is expected to be dominated by non-hadronic states. Thus, the location of the CP is indeed sensitive to the nature and magnitude of the coupling constants. In fact, it was actually found in [19] that the $U_A(1)$ anomaly strength modeled through the chemical potential dependent coupling $g_{\rm D}$ may change the curvature of the critical surface, as well as its sign, resulting in a characteristic "backbending" of the critical surface as a function of μ. This reflects the fact that the density dependence of the coupling strengths plays crucial role when investigating the chiral critical surface.

Acknowledgments

We are grateful to Ph. de Forcrand for suggesting us to perform this calculation. HK likes to thank T. Inagaki and D. Kimura for fruitful discussions. HK is supported by the grant NSC-99-2811-M-033-017 from National Science Council (NSC) of Taiwan. JWC and UR are supported by the NSC and NCTS of Taiwan. UR is also supported in part by the NSF grant of USA No. PHYS-0758114. He thanks the Institute of Mathematical Science Chennai and the Indian Institute of Technology Bombay, for their kind hospitality during the progress of this work.

[1] For a recent review on the QCD phase diagram, see: K. Fukushima and T. Hatsuda, arXiv:1005.4814 [hep-ph].

[2] M. Asakawa and K. Yazaki, Nucl. Phys. A **504**, 668 (1989); A. Barducci, R. Casalbuoni, S. De Curtis, R. Gatto, and G. Pettini, Phys. Lett. B **231**, 463 (1989); Phys. Rev. D **41**, 1610 (1990); J. Berges and K. Rajagopal, Nucl. Phys. B **538**, 215 (1999) [arXiv:hep-ph/9804233]; M. A. Halasz, A. D. Jackson, R. E. Shrock, M. A. Stephanov and J. J. M. Verbaarschot, Phys. Rev. D **58**, 096007 (1998) [arXiv:hep-ph/9804290]; Y. Hatta and T. Ikeda, Phys. Rev. D **67**, 014028 (2003) [arXiv:hep-ph/0210284].

[3] C. R. Allton et al., Phys. Rev. D **68**, 014507 (2003); Phys. Rev. D **71**, 054508 (2005); Z. Fodor and S. D. Katz, JHEP 0404, 050 (2004); Y. Aoki, Z. Fodor, S. D. Katz and K. K. Szabo, JHEP 0601, 089 (2006); F. Karsch and E. Laermann, in *Quark Gluon Plasma III*, edited by R.C. Hwa and X. N. Wang (World Scientific, Singapore, 2004), arXiv:hep-lat/0305025; O. Philipsen, Prog. Theor. Phys. Suppl. **174**, 206 (2008) [arXiv:0808.0672 [hep-ph]].

[4] P. de Forcrand, PoS **LAT2009**, 010 (2009) [arXiv:1005.0539 [hep-lat]].

[5] Y. Nambu and G. Jona-Lasinio, Phys. Rev. **122**, 345 (1961); *ibid.* **124**, 246 (1961).

[6] K. Fukushima, Phys. Lett. B **591**, 277 (2004) [arXiv:hep-ph/0310121].

[7] T. Hatsuda and T. Kunihiro, Phys. Rept. **247**, 221 (1994) [arXiv:hep-ph/9401310].

[8] S. P. Klevansky, Rev. Mod. Phys. **64**, 649 (1992).

[9] M. Buballa, Phys. Rept. **407**, 205 (2005)

[10] K. Fukushima, Phys. Rev. D **77**, 114028 (2008) [Erratum-ibid. D **78**, 039902 (2008)] [arXiv:0803.3318 [hep-ph]].

[11] R. D. Pisarski and F. Wilczek, Phys. Rev. D **29**, 338 (1984).

[12] P. de Forcrand, S. Kim and O. Philipsen, PoS **LAT2007**, 178 (2007) [arXiv:0711.0262 [hep-lat]]; P. de Forcrand and O. Philipsen, JHEP **0811**, 012 (2008) [arXiv:0808.1096 [hep-lat]]; G. Endrodi, Z. Fodor, S. D. Katz and K. K. Szabo, PoS **LAT2007**, 182 (2007) [arXiv:0710.0998 [hep-lat]].

[13] O. Philipsen, arXiv:0910.0785 [hep-ph].

[14] J. W. Chen, K. Fukushima, H. Kohyama, K. Ohnishi and U. Raha, Phys. Rev. D **81**, 071501 (2010) [arXiv:0912.2099 [hep-ph]].

[15] M. Kobayashi and T. Maskawa, Prog. Theor. Phys. **44**, 1422 (1970); M. Kobayashi, H. Kondo and T. Maskawa, Prog. Theor. Phys. **45**, 1955 (1971); G. 't Hooft, Phys. Rev. Lett. **37**, 8 (1976).

[16] For the critical surface in another model, see e.g., B. J. Schaefer and M. Wagner, Phys. Rev. D **79**, 014018 (2009) [arXiv:0808.1491 [hep-ph]].

[17] C. Ratti, M. A. Thaler and W. Weise, Phys. Rev. D **73**, 014019 (2006); S. Rossner, C. Ratti and W. Weise, Phys. Rev. D **75**, 034007 (2007).

[18] This difference can also be seen in the 2 flavor case, see for example, P. Costa, C. A. de Sousa, M. C. Ruivo and H. Hansen, Europhys. Lett. **86** (2009) 31001 [arXiv:0801.3616 [hep-ph]].

[19] J. W. Chen, K. Fukushima, H. Kohyama, K. Ohnishi and U. Raha, Phys. Rev. D **80**, 054012 (2009) [arXiv:0901.2407 [hep-ph]].